CONSTRAINTS ON THE EMISSION MODEL OF THE "NAKED-EYE BURST" GRB 080319B

A. A. Abdo[1,2], A. U. Abeysekara[1], B. T. Allen[3,16], T. Aune[4,17], D. Berley[5], C. Chen[3,18], G. E. Christopher[6,19],
T. DeYoung[7], B. L. Dingus[8], R. W. Ellsworth[2], M. M. Gonzalez[9], J. A. Goodman[5], J. Granot[10], E. Hays[11],
C. M. Hoffman[8], P. H. Hüntemeyer[12], B. E. Kolterman[6], J. T. Linnemann[1], J. E. McEnery[11], A. I. Mincer[6],
T. Morgan[13], P. Nemethy[6], J. Pretz[8], E. Ramirez-Ruiz[14], J. M. Ryan[13], P. M. Saz Parkinson[4], A. Shoup[15], G. Sinnis[8],
A. J. Smith[5], V. Vasileiou[5,20], G. P. Walker[8,21], D. A. Williams[4], and G. B. Yodh[3]

[1] Department of Physics and Astronomy, Michigan State University, 3245 BioMedical Physical Sciences Building, East Lansing, MI 48824, USA
[2] School of Physics, Astronomy and Computational Sciences, George Mason University, Fairfax, VA 22030, USA
[3] Department of Physics and Astronomy, University of California, Irvine, CA 92697, USA
[4] Santa Cruz Institute for Particle Physics, University of California, 1156 High Street, Santa Cruz, CA 95064, USA
[5] Department of Physics, University of Maryland, College Park, MD 20742, USA
[6] Department of Physics, New York University, 4 Washington Place, New York, NY 10003, USA
[7] Department of Physics, Pennsylvania State University, University Park, PA 16802, USA
[8] Group P-23, Los Alamos National Laboratory, P.O. Box 1663, Los Alamos, NM 87545, USA
[9] Instituto de Astronomía, Universidad Nacional Autónoma de México, D.F., México 04510, Mexico
[10] The Open University of Israel, 1 University Road, POB 808, Ra'anana 43537, Israel
[11] NASA Goddard Space Flight Center, Greenbelt, MD 20771, USA
[12] Department of Physics, Michigan Technological University, Houghton, MI 49931, USA
[13] Department of Physics, University of New Hampshire, Morse Hall, Durham, NH 03824, USA
[14] Department of Astronomy and Astrophysics, University of California, Santa Cruz, CA 95064, USA
[15] Department of Physics, The Ohio State University, Lima, OH 45804, USA

ABSTRACT

On 2008 March 19, one of the brightest gamma-ray bursts (GRBs) ever recorded was detected by several ground- and space-based instruments spanning the electromagnetic spectrum from radio to gamma rays. With a peak visual magnitude of 5.3, GRB 080319B was dubbed the "naked-eye" GRB, as an observer under dark skies could have seen the burst without the aid of an instrument. Presented here are results from observations of the prompt phase of GRB 080319B taken with the Milagro TeV observatory. The burst was observed at an elevation angle of 47°. Analysis of the data is performed using both the standard air shower method and the scaler or single-particle technique, which results in a sensitive energy range that extends from ∼5 GeV to >20 TeV. These observations provide the only direct constraints on the properties of the high-energy gamma-ray emission from GRB 080319B at these energies. No evidence for emission is found in the Milagro data, and upper limits on the gamma-ray flux above 10 GeV are derived. The limits on emission between ∼25 and 200 GeV are incompatible with the synchrotron self-Compton model of gamma-ray production and disfavor a corresponding range (2 eV–16 eV) of assumed synchrotron peak energies. This indicates that the optical photons and soft (∼650 keV) gamma rays may not be produced by the same electron population.

Key words: astroparticle physics – gamma-ray burst: individual (GRB 080319B)

Online-only material: color figure

1. INTRODUCTION

On 2008 March 19 one of the brightest gamma-ray bursts (GRBs) to date was detected by the Burst Alert Telescope (BAT) on board *Swift* (Cummings et al. 2008) and by the Konus GRB spectrometer on board the *Wind* spacecraft (Golenetskii et al. 2008). Due in part to the burst's proximity (10° separation) to GRB 080319A, which was detected <30 minutes earlier, the prompt phase of GRB 080319B was observed in the optical band by several wide-field robotic optical telescopes (Bloom et al. 2009 and references therein). With a measured redshift of $z = 0.937$ (Vreeswijk et al. 2008), this is the most distant

astronomical object known to be observable with the naked eye. The unusually good broadband coverage of the prompt emission from GRB 080319B provided a unique scenario for testing models of gamma-ray emission from internal shocks (Zou et al. 2009a, 2009b; Yu et al. 2009) as well as alternative emission scenarios (Kumar & Narayan 2009). Contemporaneous gamma-ray and optical data for GRB 080319B appear to be at least mildly correlated, leading to the conclusion that both the optical and gamma-ray emission are likely produced in the same physical region (Racusin et al. 2008). Perhaps the most natural explanation of the observed emission of GRB 080319B comes from the synchrotron self-Compton (SSC) model.

The SSC interpretation in the context of correlated optical and gamma-ray emission and a strong first order inverse Compton (IC) peak, as observed in the case of GRB 080319B, predicts a strong second order IC peak in the hundreds of GeV (Kumar & Panaitescu 2008), within the energy range and sensitivity of the Milagro gamma-ray observatory (Atkins et al. 2004). GRB 080319B occurred in the Milagro field of view at an elevation angle of 47°. Analyses of the Milagro data during

the prompt phase of GRB 080319B using two independent techniques show no indication of gamma-ray emission. Taking into account the gamma-ray attenuation by the extragalactic background light (EBL), the upper limits on the >20 GeV emission obtained with Milagro fall below the theoretically predicted flux from the second order IC peak in the SSC model, assuming that this second order IC peak lies between 25 and 200 GeV.

2. THE MILAGRO OBSERVATORY

Milagro was a water-Cherenkov extensive-air-shower array located in the Jemez mountains (2630 m a.s.l.) near Los Alamos, New Mexico, U.S.A. (35°.9 N, 106°.7 W) and was operational from 2000 January until 2008 May. The main detector consisted of a central pond of highly purified water instrumented with 723 photomultiplier tubes (PMTs). The top (air-shower) layer, ∼1.5 m below the surface, was used for angular reconstruction while the bottom (muon) layer, ∼6 m below the surface, was used for gamma/hadron separation. In 2004, an array of 175, 4000 liter water tanks, each instrumented with a single PMT, was added around the central pond, increasing the area of the detector and allowing for improved gamma/hadron separation. Milagro had a field of view of ∼2 sr and a duty cycle greater than 90%, making it an effective all-sky monitor of transient phenomena, like GRBs, at GeV–TeV energies. Previous searches for very high energy (VHE; >100 GeV) emission from GRBs with Milagro have yielded no conclusive detections (Atkins et al. 2005; Abdo et al. 2007; Saz Parkinson 2009).

3. DATA ANALYSIS

Milagro simultaneously recorded data from two parallel data acquisition systems: reconstructed shower events and scaler count rates. Data from both systems were used to obtain independent upper limits on the gamma-ray flux from GRB 080319B. In this section, a brief description of the analysis method used for each set of data is given below.

3.1. Standard Analysis

For energies >50 GeV, the Milagro standard air-shower analysis is used to search for an excess of events above the expected background, temporally and positionally coincident with the main gamma-ray pulse of GRB 080319B as detected by Konus. An estimate of the number of background events is made by characterizing the angular distribution of the background using 2 hr of data surrounding the burst, as described in Atkins et al. (2003). The total number of events falling within a circular bin of radius 1°.6 centered on the burst is summed over the duration of the burst. The significance of the excess (or deficit) of the burst is evaluated using Equation (17) of Li & Ma (1983). Given the observed on-source counts and the predicted background, the 99% confidence upper limits on signal counts are computed using the Helene prescription (Helene 1983).

3.2. Scaler Analysis

In parallel with acquiring data from reconstructed air shower events, Milagro also recorded the hit rates of all of the Milagro PMTs once per second. Although the direction and energy of individual primary gamma rays cannot be reconstructed with these data, a statistically significant increase in the scaler rate will accompany a sufficiently large increase in the flux of gamma rays incident on the upper atmosphere. Consequently, the scaler

data can be used to search for gamma-ray emission from GRBs using the temporal information from satellite-based gamma-ray detectors. The scaler analysis method offers a significant improvement to the effective area of Milagro at low (<50 GeV) energies over the standard air shower analysis described above.

The Milagro scaler data acquisition and analysis is implemented as follows: The PMTs in the Milagro pond are grouped into non-neighboring sets of eight and the hit rate of the logical "or" for each set is recorded every second. The PMT rates are recorded simultaneously at both low (∼0.25 photoelectrons) and high (∼4 photoelectrons) thresholds. The results presented here are obtained using the low-threshold rates of the upper (air-shower) layer of PMTs as it has the lowest energy threshold of the Milagro arrays. Details on the PMT layout and grouping in the scaler system are similar to those for Milagrito, and can be found in Atkins et al. (2003).

The first step in the analysis of the raw scaler data is the exclusion of noisy "or"-groups. Noisy groups can arise for several reasons, including light leaks or water seeping into the PMT electronics. The exclusion is done by calculating the root mean square (rms) of the rate from each "or"-group over the ±5 day time period surrounding the burst. Groups with an rms that degrades the signal to noise ratio of the sum of all the "or"-groups are considered noisy, and are excluded from the analysis. The next step is the correction of the variation in the rates due to pressure and temperature fluctuations of the outside environment. Linear corrections for both outside temperature and atmospheric pressure which minimize the rms of the rate are calculated for the same ±5 day time period. Corrections based on electronics temperature were investigated but were not found to improve the sensitivity, i.e., reduce the rms of the scaler rates, and are neglected here.

Finally, the average count rate during the GRB is compared to the average background rate five minutes (5×GRB duration) before and after the burst itself. This comparison is also done for 1500 similar 11 minute duration test intervals over the ∼11 day period surrounding the burst. It is observed that the fluctuations are neither Poissonian nor Gaussian so the statistical significance of the burst interval cannot be directly computed from these data. The difference in the counting rate between the burst region and the background region is compared to the rate differences in the test intervals to obtain the significance of the count rate difference and the 99% confidence upper limits on the rate. Determining the significance of the count rate is done by computing the Gaussian σ which corresponds to the probability that the counting rate is a background fluctuation, while the upper limit is determined by computing the amount of signal that must be added to the test intervals so that 99% of them have a larger excess than the GRB interval. More details on the GRB scaler analysis procedure can be found in Aune (2012).

4. RESULTS

In the field of view of Milagro, GRB 080319B was located at an elevation angle of ∼47°. For the results presented here, the prompt phase of GRB 080319B is considered to begin at $T_0 = 22370.339$ s (06:12:50.339) UT and extend for a duration of 60 s; both quantities were selected based on the main pulse observed by the Konus instrument (Golenetskii et al. 2008). In the standard analysis, Milagro observed 30 events during this burst interval, with a predicted background of 29.7 events. This gives a 99% confidence-level upper limit of 17.3 events.
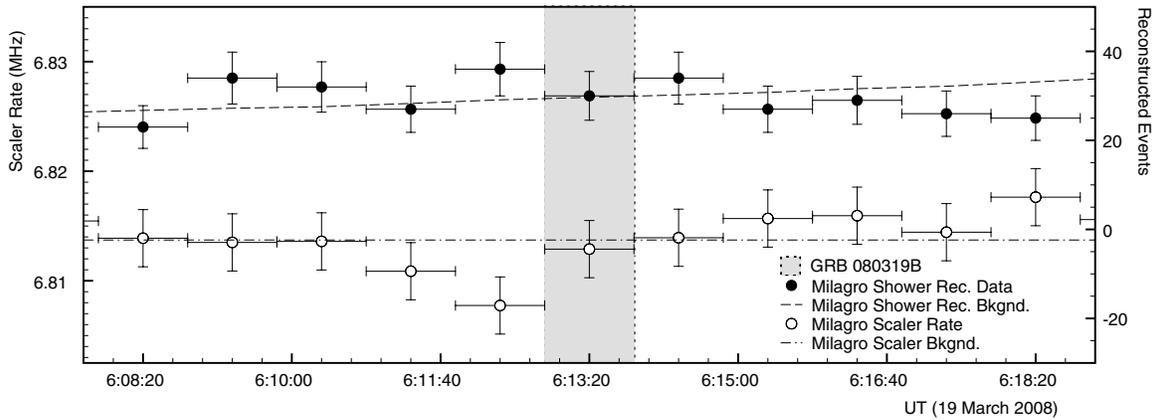
Figure 1. Light curve of both the scaler and reconstructed air shower count rates coincident with GRB 080319B and the time immediately before and after the prompt phase of the burst. The light curve is binned in intervals of the burst duration, which for GRB 080319B was 60 s. No significant excess of events associated with the prompt phase of GRB 080319B is observed.

The scaler analysis of the data collected coincident with GRB 080319B shows no significant excess in the scaler count rate associated with the prompt phase of the burst. Using the scaler analysis procedure described in Section 3.2, a 0.35σ deficit with respect to the background rate is found in the Milagro data during the time interval coincident with the main gamma-ray pulse observed by the Konus instrument. This results in a 99% confidence-level upper limit on the scaler rate of 11.8 kHz. The Milagro light curves obtained from both the scaler and standard analyses are shown in Figure 1.

To calculate the corresponding upper limit on the photon flux above some threshold energy, E_{th}, a monochromatic GRB spectrum at the threshold energy is assumed. Because the sensitivity of Milagro improves with energy, this procedure gives the most conservative limit on the integral flux above E_{th}. We assume an attenuation of the gamma-ray burst spectrum by the EBL according to the model of Gilmore et al. (2009). The effective area of Milagro is computed via Monte Carlo methods for both the scaler and standard analyses using CORSIKA air shower simulations (Heck et al. 1998) and a GEANT4-based (Agostinelli et al. 2003) instrument model. The simulations are described in Atkins et al. (2005). With the effective area, EBL-attenuated GRB spectrum, and an upper limit on events, an upper limit on the integral photon flux above various values of E_{th} is calculated. These limits are shown for both the standard analysis and the scaler analysis in Figure 2. For the monochromatic spectral assumption, the scaler upper limits extend to significantly lower energies than the standard analysis upper limits, and that the upper limits are comparable below $\sim$100 GeV. For a source with significant emission extending below 100 GeV and suffering attenuation from the EBL at higher energies, as is presumed for GRB 080319B, the scaler analysis provides better overall sensitivity than the standard analysis. We proceed, then, using the upper limits obtained with the scaler analysis to constrain the emission from GRB 080319B in the results discussed below.

In addition to calculating upper limits on the conservative, but rather non-physical, assumption of a monochromatic GRB spectrum, a more realistic spectral hypothesis can be used. If one assumes that the optical emission detected during the prompt phase of GRB 080319B is due to synchrotron radiation from a population of energetic electrons and that the keV–MeV gamma rays detected by Konus arise from IC scattering of these synchrotron photons by this same population of electrons, it follows that gamma rays with energies in the tens to hundreds
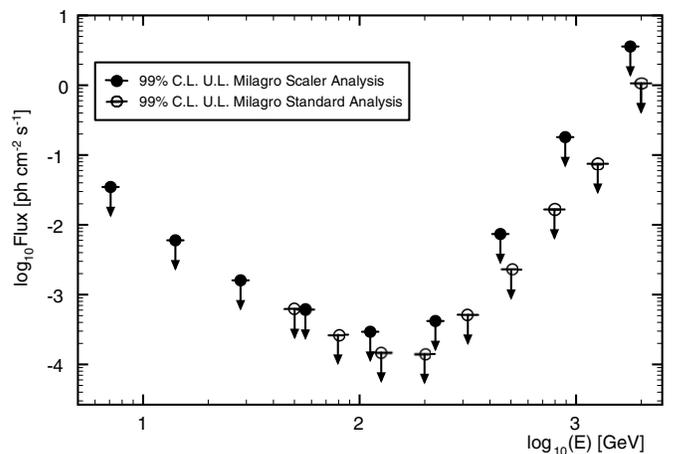
Figure 2. 99% confidence-level upper limits on the integral photon flux above various values of E_{th} assuming a monochromatic (δ-function) intrinsic GRB spectrum at E_{th} (see text for details). This spectrum is then attenuated by the EBL using the model of Gilmore et al. (2009). The upper limits from both the scaler and standard analyses are plotted here.

of GeV should be produced by secondary IC scattering of the keV–MeV gamma rays (Figure 3). The shape of this high-energy, second-order spectral feature should resemble that of the keV–MeV spectrum, which is fit well by a Band function (Band et al. 1993) with spectral indices $\alpha = -0.833$, $\beta = -3.499$ (Racusin et al. 2008). Using the measurement from the wide-field optical instrument TORTORA (Beskin et al. 2010) as an anchor point, we assume several synchrotron spectra, again with a Band function form with $\alpha = -0.833$, $\beta = -3.499$, with $0.4\,\mathrm{eV} \leqslant E_{p,\mathrm{sync}} \leqslant 40\,\mathrm{eV}$, where $E_{p,\mathrm{sync}}$ is the Band function peak energy of the synchrotron spectrum. According to the SSC model, each of these assumed synchrotron spectra, in the context of the keV–MeV peak, gives rise to a corresponding Band-function spectral feature in the GeV energy range that could be detected with Milagro. Using this GeV-Band function as the spectral assumption together with the 99% confidence-level upper limits on the scaler count rate from Milagro, we calculate the corresponding limit on νF_ν at the GeV Band function peak energy ($E_{p,\mathrm{GeV}}$) for several different values of $E_{p,\mathrm{sync}}$. These limits are shown in Figure 3 together with the average flux observed by TORTORA (Racusin et al. 2008) and the gamma-ray spectrum obtained with Konus. The Milagro upper limits are computed assuming attenuation of the high-energy
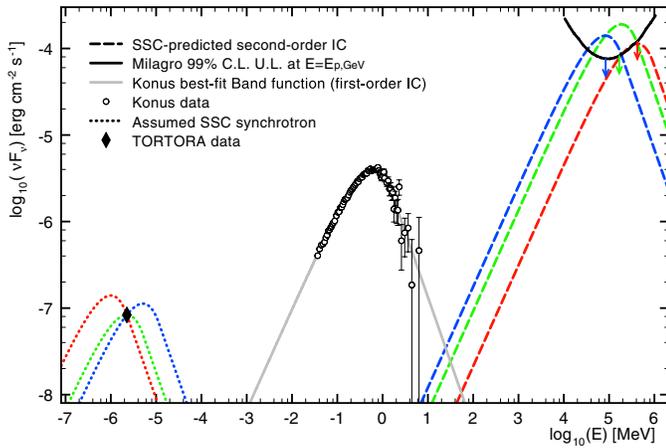
Figure 3. 99% confidence-level scaler upper limits on the prompt νF_ν flux obtained using the scaler analysis method described in the text. The limits are quoted at $E = E_{p,GeV}$ where $E_{p,GeV}$ is the peak energy for various intrinsic Band-function GRB spectra. Also shown are the data obtained simultaneously by Konus and TORTORA. The dotted lines show three assumed synchrotron spectra ($E_{p,syn} = 1, 2.26, 5.1$ eV). The peak of the synchrotron spectrum relative to the peak of the keV–MeV spectrum sets the value of the Compton parameter, Y. The corresponding second-order IC spectral features predicted by the SSC model, assuming $Y_2 = Y$ are shown with dashed lines. The Milagro upper limits are compared to the unattenuated second-order IC spectral components since the limits plotted here already account for gamma-ray attenuation from both Klein–Nishina suppression and attenuation via pair production with the EBL.
(A color version of this figure is available in the online journal.)

gamma rays by both Klein–Nishina suppression at the source and by the intervening EBL based on the model of Gilmore et al. (2009).

From the observations of GRB 080319B by Konus and TORTORA, a Compton parameter of $Y \lesssim 100$ is found, with this parameter being defined as the ratio between the amount of energy carried in the first-order IC (keV–MeV gamma ray) component and the synchrotron (optical) component. Assuming that the SSC mechanism is responsible for the emission observed in the optical and keV–MeV gamma-ray bands and following the discussion in Kumar & Panaitescu (2008), it is predicted that there should exist a second-order IC spectral feature and that it should peak at $\sim400(\nu_{io}/1\,\text{eV})^{-1}$ GeV ($\nu_{io} \lesssim 1$ eV being the peak of the synchrotron spectrum) and carry a fluence of $Y_2 = Y = 100$ times that carried in the first-order IC (i.e., Konus-detected) component. The upper limits obtained by Milagro indicate that $Y_2 \leqslant 20$, a factor of five less than predicted.

5. DISCUSSION

This result is the only direct experimental constraint on the SSC mechanism and strongly disfavors this scenario in the case of GRB 080319B assuming the GeV peak lies in the ~25–200 GeV energy range. These Milagro upper limits relative to predicted fluxes are illustrated in Figure 4 where the scaler 99% confidence-level upper limits at various $E_{p,GeV}$ are plotted with the predicted SSC-model-predicted flux at $E_{p,GeV}$. In deriving these limits, the assumed GRB spectrum is a Band function with peak energies $E_{p,GeV} = E_{p,IC2}$ varying between 10 GeV and 1 TeV, which is then attenuated due to Klein–Nishina suppression assuming a bulk Lorentz factor $\Gamma = 500$.

This spectrum is assumed to be further attenuated at high energies due to interaction with the EBL. The upper limits, then, are limits on the unattenuated predicted fluxes of the second
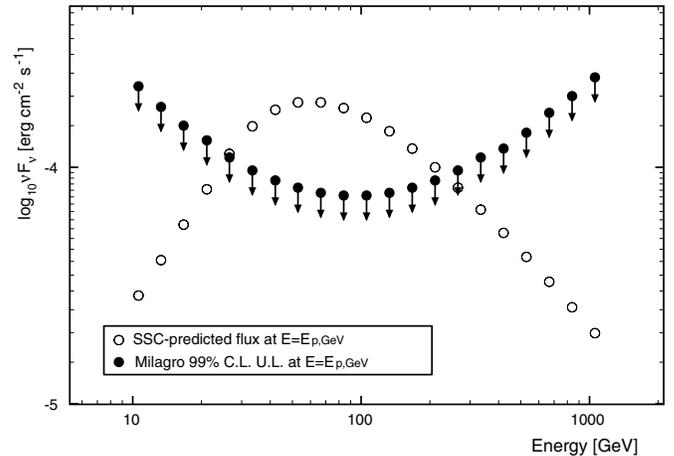
Figure 4. SSC-model-predicted prompt νF_ν flux at $E = E_{p,GeV}$ (open points) plotted for several assumed values of $E_{p,GeV}$ and the corresponding 99% confidence-level upper limits obtained with Milagro using the scaler method described in the text (filled points). The Milagro limits account for attenuation of the high-energy gamma-ray flux by both Klein–Nishina suppression at the source and from the EBL using the model of Gilmore et al. (2009).

order IC peak and are compared with these fluxes in Figure 4. In turn, the synchrotron peak energy, $E_{p,syn}$ can be determined by the energy of the first and second order IC peak energies ($E_{p,IC}$, $E_{p,IC2}$) in the SSC model through $E_{p,syn} \approx E_{p,IC1}^2/E_{p,IC2}$, where $E_{p,IC1}$ is the peak of the Band function measured by Konus. Since Milagro limits exclude the 25–200 GeV peak energies of the second order IC component, the corresponding $E_{p,syn}$ in the 2–16 eV range is equivalently excluded.

Due to the apparent correlation in time and different spectral properties of the optical and gamma-ray emission from GRB 080319B (i.e., the extrapolation of the gamma-ray spectrum to lower energies under-predicts the optical emission by several orders of magnitude), the SSC model offers a "natural" explanation but is not without problems. One such problem is that the first-order IC spectrum is predicted to follow $F_\nu \propto \nu$ below the self-absorbed photon energy ($\sim$100 keV) whereas a significantly softer spectrum $F_\nu \propto \nu^{0.2}$ was measured by Konus. Considering the constraints from synchrotron self-absorption in GRB 080319B, Zou et al. (2009b) show that for reasonable assumptions of the bulk Lorentz factor ($\Gamma \sim 500$–1000), small values ($\lesssim$30) of the Compton parameter Y are forbidden. On the other hand, the Milagro upper limits presented here serve to directly rule out the possibility of large values of Y. Consequently, the SSC model cannot explain the observed properties of GRB 080319B. However, if one instead supposes that the prompt optical and gamma-ray photons are produced in separate physical regions (i.e., not correlated), then the observed spectra may be reproduced while additionally allowing for a reasonable, but not extreme high-energy component (Zou et al. 2009a). Furthermore, it may be possible to explain the emission from GRB 080319B without invoking the internal shock model at all but rather by assuming a turbulent source near the deceleration radius of the outflow (Kumar & Narayan 2009).

6. CONCLUSIONS

GRB 080319B had the highest optical luminosity and one of the highest gamma-ray fluences of any GRB yet detected. The extremely bright optical component and proximity to GRB 080319A led to GRB 080319B being one of the most observationally well-covered GRBs to date. The unique qualities

of GRB 080319B, particularly the intensity of optical emission associated with the prompt phase of the event, challenge some of the standard theoretical models of GRBs. Perhaps the most natural explanation of the emission detected from GRB 080319B is provided by the SSC model, where the gamma rays and optical photons are produced in the same physical region. Such a model, however, predicts the existence of a bright spectral peak in the tens to hundreds of GeV, within the energy range and sensitivity of the Milagro detector. The Milagro data associated with GRB 080319B show no significant gamma-ray signal using either the standard air-shower or scaler analyses. The resulting upper limits on the gamma-ray flux constrain the second order Compton parameter, Y_2, to be well below that predicted by the SSC model across a broad range of energies, disfavoring this scenario in these cases. This result is the only direct experimental constraint on the high-energy emission from GRB 080319B and demonstrates the power of a large-area, wide field of view, continuously operating VHE observatory with respect to GRB observations. A next-generation extensive air shower array dubbed the High Altitude Water Cherenkov (HAWC) observatory is currently under construction and is expected to provide a 15-fold increase in sensitivity compared to that of Milagro (Abeysekara et al. 2012). It is predicted that HAWC could detect GRBs with characteristics similar to some *Fermi*-LAT-detected bursts, e.g., GRB 090510 (De Pasquale et al. 2010) and GRB 090902B (Abdo et al. 2009), and information provided by HAWC on the high-energy spectra of GRBs could greatly improve our understanding of GRB physics.

REFERENCES

Abdo, A. A., Ackermann, M., Ajello, M., et al. 2009, ApJ, 706, L138
Abdo, A. A., Allen, B. T., Berley, D., et al. 2007, ApJ, 666, 361
Abeysekara, A. U., Aguilar, J. A., Aguilar, S., et al. 2012, Astropart. Phys., 32, 641
Agostinelli, S., Allison, J., Amako, K., et al. 2003, Nucl. Instrum. Methods Phys. Res. A, 506, 250
Atkins, R., Benbow, W., Berley, D., et al. 2003, ApJ, 583, 824
Atkins, R., Benbow, W., Berley, D., et al. 2004, ApJ, 608, 680
Atkins, R., Benbow, W., Berley, D., et al. 2005, ApJ, 630, 996
Aune, T. 2012, PhD thesis, University of California, Santa Cruz
Band, D., Matteson, J., Ford, L., et al. 1993, ApJ, 413, 281
Beskin, G., Karpov, S., Bondar, S., et al. 2010, ApJ, 719, L10
Bloom, J. S., Perley, D. A., Li, W., et al. 2009, ApJ, 691, 723
Cummings, J., Barthelmy, S. D., Fenimore, E., et al. 2008, GCN, 7462, 1
De Pasquale, M., Schady, P., Kuin, N. P. M., et al. 2010, ApJ, 709, L146
Gilmore, R. C., Madau, P., Primack, J. R., Somerville, R. S., & Haardt, F. 2009, MNRAS, 399, 1694
Golenetskii, S., Aptekar, R., Mazets, E., et al. 2008, GCN, 7482, 1
Heck, D., Knapp, J., Capdevielle, J. N., Schatz, G., & Thouw, T. 1998, CORSIKA: a Monte Carlo Code to Simulate Extensive Air Showers (Karlsruhe: Forschungszentrum Karlsruhe GmbH)
Helene, O. 1983, Nucl. Instrum. Methods Phys. Res., 212, 319
Kumar, P., & Narayan, R. 2009, MNRAS, 395, 472
Kumar, P., & Panaitescu, A. 2008, MNRAS, 391, L19
Li, T., & Ma, Y. 1983, ApJ, 272, 317
Racusin, J. L., Karpov, S. V., Sokolowski, M., et al. 2008, Nature, 455, 183
Saz Parkinson, P. M. 2009, in AIP Conf. Proc. 1112, Science with the New Generation of High Energy Gamma-Ray Experiments, ed. D. Bastieri & R. Rando (Melville, NY: AIP), 181
Vreeswijk, P. M., Smette, A., Malesani, D., et al. 2008, GCN, 7444, 1
Yu, Y. W., Wang, X. Y., & Dai, Z. G. 2009, ApJ, 692, 1662
Zou, Y.-C., Fan, Y.-Z., & Piran, T. 2009a, MNRAS, 396, 1163
Zou, Y.-C., Piran, T., & Sari, R. 2009b, ApJ, 692, L92